INTERFACE

rsif.royalsocietypublishing.org

Research

Cite this article: Chelakkot R, Mahadevan L. 2017 On the growth and form of shoots. *J. R. Soc. Interface* **14**: 20170001. http://dx.doi.org/10.1098/rsif.2017.0001

Received: 1 January 2017
Accepted: 21 February 2017

Subject Category:
Life Sciences–Physics interface

Subject Areas:
biomechanics, biophysics, systems biology

Keywords:
growth and form, plant shoots, gravitropism, mathematical model

Author for correspondence:
L. Mahadevan
e-mail: Lmahadev@g.harvard.edu

Electronic supplementary material is available at https://dx.doi.org/10.6084/m9.figshare.c.3708364.

THE ROYAL SOCIETY PUBLISHING

On the growth and form of shoots

Raghunath Chelakkot[1,4] and L. Mahadevan[1,2,3]

[1]Paulson School of Engineering and Applied Sciences, [2]Department of Organismic and Evolutionary Biology, and [3]Department of Physics, Wyss Institute for Biologically Inspired Engineering, Kavli Institute for Nano-bio Science and Technology, Harvard University, Cambridge, MA 02138, USA
[4]Department of Physics, Indian Institute of Technology Bombay, Mumbai 400076, India

LM, 0000-0002-5114-0519

Growing plant stems and shoots exhibit a variety of shapes that embody growth in response to various stimuli. Building on experimental observations, we provide a quantitative biophysical theory for these shapes by accounting for the inherent observed passive and active effects: (i) the active controllable growth response of the shoot in response to its orientation relative to gravity, (ii) proprioception, the shoot's growth response to its own observable current shape, and (iii) the passive elastic deflection of the shoot due to its own weight, which determines the current shape of the shoot. Our theory separates the sensed and actuated variables in a growing shoot and results in a morpho-space diagram in terms of two dimensionless parameters representing a scaled local active gravitropic sensitivity, and a scaled passive elastic sag. Our computational results allow us to explain the variety of observed transient and steady morphologies with effective positive, negative and even oscillatory gravitropic behaviours, without the need for ad hoc complex spatio-temporal control strategies in terms of these parameters. More broadly, our theory is applicable to the growth of soft, floppy organs where sensing and actuation are dynamically coupled through growth processes via shape.

1. Introduction

The ability of plants to control growth movements in response to various environmental cues is well known [1]. These directional movements, called tropisms, enable plants to respond by orienting their growth to external stimuli. One of the most commonly observed of these movements is gravitropism, wherein plant shoots perceive the direction of gravity and regulate their growth to achieve a steady orientation with respect to gravity [2–8]. The perception of gravity occurs within specialized cells called statocytes through the sedimentation of intracellular statoliths [5,8,9] onto sensory structures. This mechanical signal leads to a differential growth across the cross section of a shoot and thence active (sentient) bending of the respective organ [5–8,10]. Thus, plant shoots are 'negatively gravitropic', preferring a vertically upward state opposing gravity, while roots are 'positively gravitropic', preferring a vertically downward posture.

While shoots of the model organism *Arabidopsis thaliana* (figure 1*b*) concur with this expectation leading to vertically upward growing stems, there are many plants which show spatio-temporally complex orientations of their shoots. For example, *Impatiens glandulifera* [11–13] can have shoots that display oscillatory curving and de-curving before converging to a vertically upward steady orientation, *Cerastium tomentosum* (figure 1*c*) and *Toxicodendron radicans* (figure 1*d*) have shoots that first grow vertically downwards before turning upwards effectively switching from being positively gravitropic to negatively gravitropic as the plant develops, *Salix alba* (figure 1*e*) exhibits an apparent positive gravitropic behaviour by growing in the direction of gravity, and *Trandescantia fluminensis* and *Oplismenus hirtellus* [14,15] also display a 'gravitropic sign reversal' suggesting a time-dependent preferential orientation.

Attempts to explain these versatile gravitropic behaviours have led to a variety of hypotheses going back more than a century [1,16]. The simplest of these, Sachs' law, states that the local rate of curvature of the growth zone responds to the orientation of the shoot, leading to a response that is strongest at regions which are

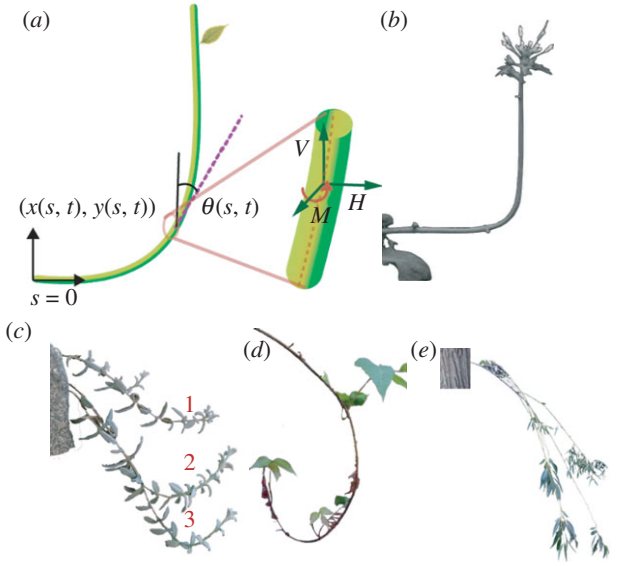

Figure 1. (*a*) Schematic of our active elastic model used to study the sentient growth of plant shoots. (*b–e*) Commonly observed gravitropic behaviour of various plant shoots. (*b*) Negative gravitropic response of *Arabidopsis thaliana* shoot [11]. (*c*) *Cerastium tomentosum* shoots of three different lengths (1–3) with axially varying gravitropic orientation. The local shoot orientation varies as the shoot length increases, suggestive of a complex control strategy. (*d*) Shoots of *Toxicodendron radicans* display axially varying gravitropic orientation with curvature reversal. (*e*) *Salix alba* shoots displaying apparent positive gravitropism. (Online version in colour.)

horizontal and weakest where it is vertical. However, this does not suffice to build a regulatory framework for stem straightening; indeed, it leads to oscillations [11] similar to those in undamped feedback control systems. Separately, evidence shows that plants and fungi have a proprioceptive sense known as autotropism that causes them to grow straight in the absence of any stimuli [3,17–20]. This straightening mechanism is not specific to the type or direction of induced stimulus and is observed whenever curvature is induced in the plant.

Independent of this literature on gravitropism and autotropism, there has also been interest in understanding the growth of plant shoots and roots from a purely mechanical perspective. By treating the growing rod as a one-dimensional continuum that can change its reference length, diameter and stiffness, various authors have formulated a theory for how its shape can vary with time [10,21–24]. A general discussion of possible evolution equations for the natural curvature has also been considered [22,25], with autotropism being the primary driver. These theoretical studies do not consider the role of multiple stimuli that include, for example, autotropic, gravitropic or phototropic responses, nor do they explore the large parameter space of variables to understand the qualitative nature of the solutions or their implications for the observed morphological diversity of plant shoots.

A recent elegant proposal by Bastien *et al*. [11,26] combines the ideas of autotropism and gravitropism into a single quantitative theory which the authors show is both necessary and sufficient to maintain a steady vertical orientation for shoots, and corroborate using a series of experiments and observations. In the minimal setting considered in [11,26], effects such as elasticity and gravity acting on soft stems, and maturation/lignification are neglected, and this implicitly raises the natural question of how to modify the theory to explain the various complex spatio-temporal morphologies of plant shoots summarized earlier.

Here, we combine these studies on gravitropism and autotropism (the sensing problem) along with the studies on mechanical growth (the actuation problem) in a minimal setting that accounts for multiple stimuli to understand a range of old observations of plant shoots. We begin by questioning the basic assumption inherent in prior models, that (proprioceptive) sensing and actuation (via growth) act on the same variable, the shape of the growth zone. While this is certainly true in a gravity-free environment, this cannot be true in general since the plant droops due to its own weight even as it grows, so that the observable shape associated with a heavy, sagging shoot and the controllable growth rate that determines the intrinsic curvature are fundamentally different objects. Building on this, we propose an observationally rooted biophysical model that combines the effects of the passive elastic deflection of soft plant shoots due to gravity, active gravitropic and proprioceptive growth acting on the deformed shoot, coupled with axial elongation in the growth zone. Our study shows that this model suffices to explain various gravitropic reorientations observed across a range of plant shoots, without the need for ad hoc control strategies for shoot growth rates in space and time.

2. Theoretical model

Gravitropic movements in most plant species are confined to a plane defined by the shoot axis and the gravity vector [1,3]. Therefore, we limit ourselves to a planar description that captures the main characteristics of the observed phenotypes, modelling the plant shoot as a thin inextensible elastic filament. At a given instant of time t, the centreline $[x(s, t), y(s, t)]$ (figure 1*a*) is parametrized by the arc length $s \in [0, \ell(t)]$, with the initial length $\ell(0) \equiv \ell_0$. We assume that the plant shoot has a bending rigidity $B(s, t)$ which can change as the shoot lignifies, and that its weight per unit length is ρg, where ρ is the linear density of the shoot. The shape of the filament is characterized by the angle $\theta(s, t)$ between the local tangent and the vertical axis (figure 1*a*).

We assume that initially the straight filament is oriented along the horizontal axis, with the basal end of the filament ($s = 0$) being horizontally clamped, with $\theta(0) = -\pi/2$, $x(0) = y(0) = 0$, while the apical end ($s = \ell$) is free. The primary growth process in shoots, including elongation and tropical bending, takes place only in the growth zone of the shoot, a localized region extending over a finite length ℓ_g from the apex [3,11] that grows uniformly at a rate $\dot{\mathcal{L}}_0$. Then, for an infinitesimal segment of length $\Delta(s)$ in this zone, we may write

$$\frac{\partial \Delta}{\partial t} = \dot{\mathcal{L}}(s)\Delta, \tag{2.1}$$

where

$$\left.\begin{aligned} \dot{\mathcal{L}}(s) = \dot{\mathcal{L}}_0 \quad & \text{if } s \in [\ell - \ell_g, \ell], \\ = 0 \quad & \text{if } s \in [0, \ell - \ell_g]. \end{aligned}\right\} \tag{2.2}$$

In the growth zone, the local intrinsic curvature $\kappa^*(s)$ is modified by active bending of the shoot which responds via local gravitropism and autotropism. A number of empirical studies have verified that the rate of gravitropic curvature change depends on the local orientation of the segment via the relation $\partial \kappa^*(s, t)/\partial t \propto \sin\theta$ [3,4]. Opposing this curvature change, a proprioceptive mechanism acts to maintain local straightness. Indeed, it has been observed [17,19] that this straightening mechanism acts in response to an induced

curvature, irrespective of its cause, i.e. $\partial\kappa^*(s,t)/\partial t \propto -\kappa$. Then the total rate of change of intrinsic curvature inside the growth zone is given by the sum of these contributions and reads

$$\frac{\partial \kappa^*}{\dot{\mathcal{L}}_0\,\partial t} = -\beta \sin\theta - \gamma\kappa. \tag{2.3}$$

Here the gravitropic sensitivity is β, while the proprioceptive sensitivity is γ. We have rescaled all rates by $\dot{\mathcal{L}}_0$, a parameter that sets the natural (inverse) time scale for growth. The balance between gravitropic sensitivity and proprioception leads to the definition of a characteristic sensitivity length, $\ell_s = \gamma/\beta$ over which these processes compete with each other [11]. We note that the proprioceptive term acts on the current curvature of the shoot, κ, which is generally different from the intrinsic curvature of the shoot κ^* when $\rho g \neq 0$. It is the presence of this term that couples the current morphology of the shoot which is determined by elasticity and gravity to the sentient growth of the shoot that changes its intrinsic curvature. In the weightless limit $\kappa = \kappa^*$, and the dynamics of shoot curvature in the growth zone is entirely determined by (2.3), and we recover the proposal of [11] leading to a single equation for the dynamics of growth. However, for soft, heavy, immature growing shoots, characteristic of real plants, we must account for gravity-induced deformation and the inability of the plant to sense its intrinsic (gravity-free) shape, coupling the physics of the growing, deforming shoot to the control law (2.3).

Since the time scale for elastic equilibrium is much shorter than the time scale for growth [2], elastic equilibrium governs the shape of the filament at all times. Local torque balance yields

$$\frac{\partial M}{\partial s} + H\sin\theta - V\cos\theta = 0, \tag{2.4}$$

where $M = B(\kappa - \kappa^*)$ and B is the bending rigidity of the filament, $\kappa = \partial\theta/\partial s$ is the actual local curvature, κ^* is the local intrinsic curvature (in the absence of any external loading). Similarly, local force balance yields

$$\frac{\partial H}{\partial s} = 0 \quad \text{and} \quad \frac{\partial V}{\partial s} = \rho g, \tag{2.5}$$

where H and V are, respectively, the horizontal and vertical force components (figure 1*a*), and ρg is the gravitational body force in the y-direction on the filament of linear density ρ due to gravity g. Additionally, we have the kinematic relations

$$\cos\theta = \frac{\partial y}{\partial s} \quad \text{and} \quad \sin\theta = \frac{\partial x}{\partial s}, \tag{2.6}$$

associated with the assumption of inextensibility and unshearability of thin filaments. The associated boundary conditions for the shape of the shoot are that the basal end is clamped horizontally with $\theta(0) = -\pi/2$, $x(0) = y(0) = 0$, while the apical end is free of forces and torques so that $H(\ell) = V(\ell) = \kappa(\ell) - \kappa^*(\ell) = 0$.

Finally, we note that as stems grow, lignification outside the growth zone [27] leads to an increase in the bending rigidity with time. We model lignification using the simple law

$$\left.\begin{aligned} B(s,t) &= B_{\max} - \Delta B \exp^{-(\delta t)/\tau} && \text{if } s \in [0,\ \ell - \ell_g], \\ &= B_0 && \text{if } s \in [\ell,\ \ell - \ell_g], \end{aligned}\right\} \tag{2.7}$$

where B_0 is the uniform bending rigidity in the growth zone, $s \in [\ell - \ell_g,\ \ell]$, $\Delta B = B_{\max} - B_0$ and $B_{\max}$ is the maximum value of the bending rigidity of fully lignified wood, δt is the age of a material point outside the growth zone ($\delta t = 0$ for $s > \ell - \ell_g$), and τ^{-1} is the maturation rate. It may be useful to contrast our model with the many theoretical models for growth-induced morphological changes of plant shoots [21–25] that assume that the actual curvature tries to relax to the natural curvature. We differ by accounting for the experimentally demonstrated facts that a shoot grows to change its curvature in response to its local orientation with respect to the direction of gravity while also trying to maintain straightness [11] noting that the actual (sensed) curvature is different from the (actuated) growth curvature.

Four dimensionless parameters characterize the dynamics of the growing filament. (i) The sensitivity parameter $\mathcal{S} = \ell_g/\ell_s$ is the ratio of the size of the growth zone ℓ_g relative to the sensitivity length ℓ_s that arises from the competition between gravitropism and autotropism. For the majority of terrestrial plants, $\mathcal{S} \lesssim 10$ [11]. (ii) The passive elasticity parameter $\mathcal{E} = \ell_g/\ell_e$ is the ratio of the elasto-gravity length $\ell_e = (B/\rho g)^{1/3}$ that arises from the competition between gravity and elasticity, and the size of the growth zone. For a young plant shoot with diameter $\simeq$1 mm, Young's modulus $\simeq 10^7$ Pa, mass density $\varrho = 10^3$ kg m^{-3} [28], $\ell_g \sim 10$ cm, so that $\mathcal{E} \simeq \mathcal{O}(1)$. (iii) The maturation parameter $\dot{\mathcal{L}}_0\tau$ is associated with lignification and controlled by the relative maturation rate. In the absence of precisely quantified maturation rates in plants, we examine our model for $\dot{\mathcal{L}}_0\tau = 0.1$, 1.0 and 10, with $\mathcal{S} \in [0.5, 7]$, $\mathcal{E} = \in [0.6, 1.6]$, $B_{\max}/B_0 = 10$ and $\ell(t_0) = 0.5\ell_g - \ell_g$. (iv) Finally, the scaled growth zone size is measured relative to the initial length of the shoot $\ell_g/\ell(t_0)$. As we will see, only the first two parameters, the growth sensitivity $\mathcal{S}$ and passive elasticity $\mathcal{E}$, are relevant in determining the qualitative nature of the morphologies of growing shoots. We scale all lengths by ℓ_g and from now on depict the shape in units of the growth zone length.

Although the nonlinear system (2.4)–(2.7) has some specific limiting behaviours that may be deduced analytically in some linearized settings [11], our focus is on broadly defining the phase space of possible morphologies for which a numerical approach is more feasible. This is carried out by discretizing the filament of length ℓ into N_m nodes with position $\mathbf{r}_i$ connected by $N_m - 1$ elastic segments labelled by tangent vectors $\mathbf{b}_i = \mathbf{r}_{i+1} - \mathbf{r}_i$, such that $\sum_{i=0}^{N_m-1} |b_i| = \ell$. The growth zone of the filament is marked by the index z such that $\sum_{i=z}^{N_m-1} |\mathbf{b}_i| = \ell_g$. The tangent angle of the filament, θ_i, is defined as $\theta_i = \cos^{-1}(\mathbf{b}_i.\mathbf{e}_y/|\mathbf{b}_i|)$ and the discretized local curvature is given as $\kappa_i = (\theta_{i+1} - \theta_i)/|\mathbf{b}_i|$. The elasticity of the filament is implemented via extensional (U_e) and bending (U_b) potentials, where $U_e = (E/2)\sum_i^{N_m-1}(\mathbf{b}_i - \ell_i)^2$, ℓ_i being the equilibrium length of segment i, and $U_b = \sum_i^{N_m-2}(B_i/2)(\phi_i - \phi_i^*)^2$, where $\phi_i = \cos^{-1}((\mathbf{b}_i.\mathbf{b}_{i+1})/|\mathbf{b}_i|\,|\mathbf{b}_{i+1}|)$, and ϕ^* is the equilibrium inter-segment angle. The filament is kept practically inextensible by setting $E \gg B$. The net force acting on a node i is given by

$$\mathbf{F}_i = \nabla_{\mathbf{r}_i} U_e + \nabla_{\mathbf{r}_i} U_b - \rho g \ell_{i-1} \mathbf{e}_y. \tag{2.8}$$

The filament growth, stiffening and feedback dynamics at discretized time intervals Δt are implemented by changing the equilibrium segment lengths ℓ_i, the intrinsic curvature κ_i^* and the bending rigidity B_i using the discretized version of equations (2.1)–(2.7). For each $i > z$, ℓ_i and κ_i^* are updated using the relations $\ell_i(t + \Delta t) = \ell_i(1 + \dot{\mathcal{L}}_i)\Delta t$, $\kappa^*(t + \Delta t) = \kappa^*(t) + \dot{\mathcal{L}}\Delta t(-\beta\sin\theta_i - \gamma\kappa)$ and for every $i < z$, the bending rigidity $B_i(t + \Delta t) = B_i(t) + \Delta B(\exp(\delta t/\tau) - \exp((\delta t + \Delta t)/\tau))$.

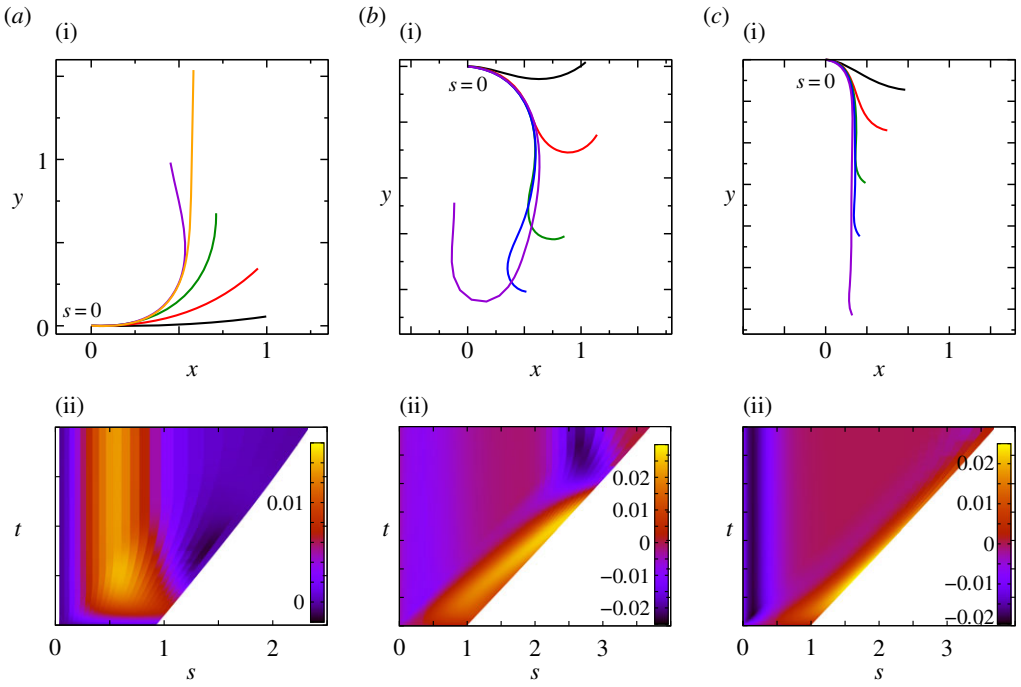

Figure 2. The time evolution of scaled shapes of a growing shoot, with different colours representing shape at different times (i). Kymographs of the local curvature (κ) as a function of arc length (s) and time (t) are shown (ii) for the sensitivity parameter $\mathcal{S} = \ell_s/\ell_g = 3$ and for various values of the elasticity parameter $\mathcal{E} = \ell_g/\ell_s$ obtained by solving equations (2.1)–(2.7). (*a*) Vertically upward growth, with negative gravitropism, and $\mathcal{E} = 0.8$, (*b*) transitional growth behaviour with an effective gravitropic 'sign reversal' and $\mathcal{E} = 1.26$, (*c*) vertically downward growth, with effective positive gravitropism, and $\mathcal{E} = 1.52$. (Online version in colour.)

As the plant shoot is always at an elastic equilibrium during the entire growth process, between each growth time step (Δt), the equilibrium shape of the filament is numerically determined using a damped Verlet method, by including the updated values of κ_i^*, ℓ_i and B_i in (2.8). This equilibrium shape provides actual values of local curvature κ_i and orientation angle θ_i which are in turn used to calculate the intrinsic shape at the next time step.

3. Growth morphologies of a sentient shoot

Although the overall morphology of sentient shoots depends on four dimensionless parameters, we find that changes in the relative maturation rate $\dot{\mathcal{L}}_0\tau$ do not significantly influence the qualitative features of the observed growth pattern (electronic supplementary material, section I and figure S1). Likewise, we also find that the observed shapes are qualitatively independent of the scaled growth zone size $\ell_g/\ell(t_0)$ (electronic supplementary material sections I–II and figure S2). Therefore, we focus on the results for $\dot{\mathcal{L}}_0\tau = 1$ and $\ell(t_0) = \ell_g$ in the rest of the paper, and study the dependence of shoot growth on the two remaining parameters: the sensitivity $\mathcal{S}$ (which can be changed by varying γ) and the elasticity $\mathcal{E}$ (which can be changed by varying ρg), for the above prescribed values of the relative maturation rates and initial length.

When $\mathcal{E} \ll 1$, corresponding to the weightless limit, the morphology of the shoot is dominated by the active bending processes determined by $\mathcal{S}$ as shown in figure 2*a*, although the steady state apex orientation is independent of $\mathcal{S}$. In this limit, when $\mathcal{S} \sim 1$ the reorientation process of the apex is monotonic (electronic supplementary material, movie S1, see the appendix for additional details). As $\mathcal{S} > 1$, i.e. when $\ell_g > \ell_s$, the filament apex overshoots the vertical, as shown in figure 2*a*(i). A kymograph of the curvature of the shoot

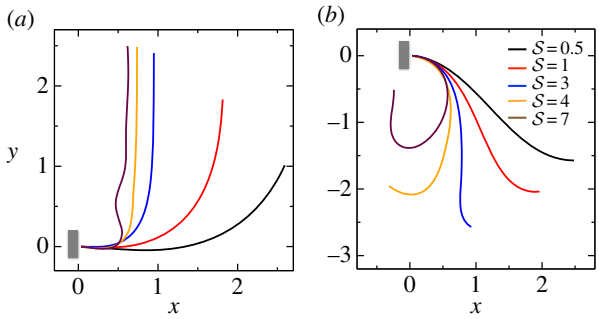

Figure 3. Scaled steady-state shapes of a growing filament for various values of the sensitivity parameter $\mathcal{S}$. Different colours represent various values of $\mathcal{S}$; from right to left $\mathcal{S} = 0.5$, 1, 3, 4 and 7 for (*a*) $\mathcal{E} = 1.0$ and (*b*) $\mathcal{E} = 1.26$. (Online version in colour.)

in figure 2*a*(ii) shows that the filament stays curved only within a limited region near the basal end. If $\mathcal{S} \gg 1$ the apex can oscillate about the vertical axis before eventually settling into a straight steady shape, again owing to proprioception. This 'weightless' limit recovers the behaviour predicted and measured by Bastien *et al.* [11] that focuses only on the dynamics of the growth zone, and is commonly observed in a number of plant species [3,11,12].

When $\mathcal{S} \gtrsim 3$ and $\mathcal{E} \sim 1$, we observe a qualitatively different gravitropic response shown in figure 2*b* (electronic supplementary material, movies S2 and S3, see the appendix for additional details). In this regime, the passive elastic deflection of the shoot due to gravity alters the local orientation angle $\theta(s)$ and thence its equilibrium shape. Because the gravitropic term in (2.3) depends on the local orientation of the shoot, the rate of curvature of the shoot changes as a result. This leads to an initial response of the shoot that is akin to negative gravitropism, since the apex is oriented vertically upward, and the

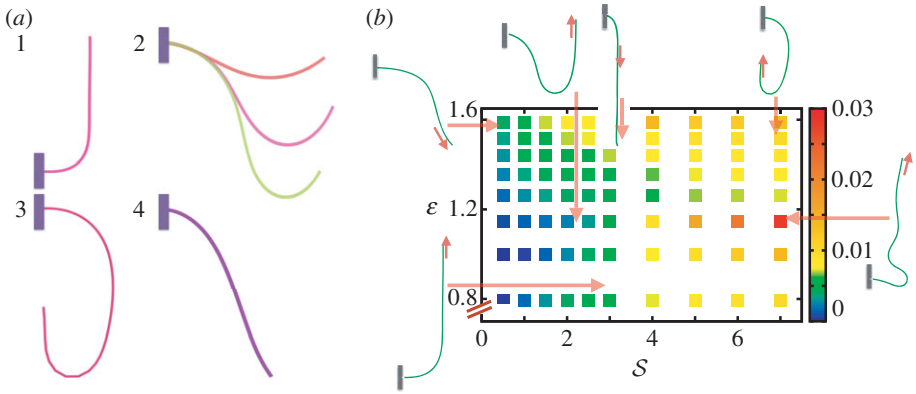

Figure 4. (*a*) The shapes obtained from the solution of our model described by equations (2.1)–(2.7) which are qualitatively similar to the shapes displayed in figure 1. (1) Negative gravitropism observed for computed shapes with $\mathcal{S} = 2.5$ and $\mathcal{E} = 0.6$. (2) Axially varying gravitropic orientation with increase in shoot length for $\mathcal{S} = 3$ and $\mathcal{E} = 1.26$. (3) Axially varying curvature change with curvature reversal, observed in our model for $\mathcal{S} = 4$ and $\mathcal{E} = 1.26$. (4) Apparent positive gravitropism for $\mathcal{S} = 0.5$ and $\mathcal{E} = 1.4$. (*b*) Morphospace for shoot shapes as a function of the sensitivity parameter $\mathcal{S} = \ell_g/\ell_s$, and the elasticity parameter $\mathcal{E} = \ell_g/\ell_e$. We note that for $\mathcal{E} < 0.8$, there are no qualitative differences from what is shown—when $\mathcal{S} \ll 1$, the shoot turns without any inflection points, while when $\mathcal{S} \gg 1$, it can have one or more points of inflection. A comparison with figure 1 shows that we can capture a range of different forms in terms of these two parameters. The colour map indicates the L_2 norm of the shoot curvature $\int_0^\ell \kappa^2(s)\,\mathrm{d}s$. (Online version in colour.)

elastic deflection in the filament is minimal. With time, the region near the base starts to orient towards gravity, while the apex favours an upward orientation (figure 2*b*(i)), that might be construed as a 'sign reversal' in gravitropism. The space–time profile of the curvature in figure 2*b*(ii) reveals that the zone of positive curvature moves towards the apex as the shoot elongates, disappearing completely as the apex straightens temporarily. Finally, the apex curves in the reverse direction and grows vertically upwards. The observed transient shapes for these intermediate values of $\mathcal{S},\mathcal{E}$ are qualitatively similar to those seen in plant species such as *Crassula ovata*, *Cerastium tomentosum* (figure 1*c*), and *Toxicodendron radicans* (figure 1*d*), and the ultimate morphology of such a shoot with reversals is similar to that observed in *Trandescantia fluminensis* and *Oplismenus hirtellus* [14,15].

For soft heavy shoots with a weak gravitropic response, passive elastic deflection dominates over gravitropic sensitivity, so that we expect the filament to orient progressively towards gravity (electronic supplementary material, movie S4, see the appendix for additional details). In figure 2*c*, we see this effective 'positive' gravitropic response for $\mathcal{E} \gtrsim 1.5$ and $\mathcal{S} \lesssim 3$. Many ornamental plant species such as *Hedera helix* or branches of some medium-sized trees such as *Salix alba* (figure 1*e*) show a negative curvature near the base and a relatively straight downward pointing apex, consistent with this scenario.

In figure 3, we show the steady shapes of shoots for different values of $\mathcal{S},\mathcal{E}$. When $\mathcal{E} = 1$, as $\mathcal{S}$ increases, negatively gravitropic shoots show a propensity for decreasing the length over which they turn, as expected, and thus also sag a little less, as seen in figure 3*a*. Furthermore, as $\mathcal{S} \gg 1$, the steady shape of the shoot has multiple inflection points in the vicinity of the base. When $\mathcal{E} > 1.2$, the orientation of the filament apex is no longer vertically upward. As shown in figure 3*b* for weak gravitropic sensitivity, i.e. $\mathcal{S} \simeq 1$, the shoot grows downwards, while when $\mathcal{S} \gtrsim 3$, the shoot eventually turns around and grows upwards.

In figure 4, we combine these observations into a shoot morphospace diagram that combines the effects of passive elasticity, active growth, gravitropism and proprioception into just two parameters: the active sensitivity $\mathcal{S}$ and the passive elasticity $\mathcal{E}$. Shoots display negative gravitropism only when the passive elastic deflection is negligible, i.e. $\mathcal{E} < 1$; an increase in $\mathcal{S}$ only changes the shoot curvature near base, but does not affect the overall morphology of the shoot. On the other hand, when $\mathcal{E} > 1$, the shoot shape can display a positive gravitropic trend with a downward orientation of the apex; this region is observed when $\mathcal{E} \gtrsim 1.2$ and $\mathcal{S} < 3$. When $\mathcal{E} \simeq 1$ and $\mathcal{S} \gtrsim 6$ the shoot displays an effective negative gravitropic trend near the apex with multiple inflection points along its length. When both effects are significant, i.e. $\mathcal{E} > 1.2$ and $\mathcal{S} > 3$, we observe a more complex regime wherein an effectively graded gravitropic preference of the shoot is seen, with points of inflection in the shape, before the shoot eventually settles into a vertical posture. A simple measure of the integrated curvature, its L_2 norm in this morphospace, shows that its maximum value corresponds to intermediate values of $\mathcal{S}$ and $\mathcal{E}$ where the shoot exhibits multiple inflection points.

4. Discussion

Our study shows that the observed diversity in the shape of plant shoots can be explained in terms of their ability to sense themselves (proprioceptively) and their environment (gravitropically) while being constrained by physical law (elasticity and gravity). In particular, our modification of the local gravitropic–proprioceptive model [11] in a simple but critical way allows us to differentiate between the controllable active growth response which acts on the natural curvature and the observable current shape. This allows us to explain effective positive, transient and negative gravitropism in plant shoots [15] in terms of two dimensionless parameters, the scaled sensitivity of growth and the scaled elasticity of the shoots.

Exploration of the solutions in this morphospace allows us to explain various gravitropic reorientations observed across a range of plant shoots, without the need for ad hoc control strategies for shoot growth rates in space and time. Our model can be easily extended to include the phototropic

responses associated with shoot reorientation just at the apex. Thus, our theory also naturally begins to set the stage for the study of decision-making in the context of multiple sensory inputs from light, gravity, proprioception, etc., in growing plant shoots. More broadly, our study also highlights how the difference between the observed shape of an organ and its controlled natural shape impacts any control law that acts on the observed shape but changes the natural shape. Indeed, the simple idea of separating the controllable actuation and observable sensing variables in growing biological systems in external fields ought to be relevant for a range of active morphogenetic events in soft growing tissues.

Competing interests. We declare we have no competing interests.

Funding. We thank the MacArthur Foundation for partial financial support.

Acknowledgments. We thank Renaud Bastien and Haiyi Liang for discussions.

References

1. Darwin C, Darwin F. 1880 *The power of movement in plants*. London, UK: Murray.
2. Gilory S, Masson PH. 2008 *Plant tropisms*. Oxford, UK: Blackwell.
3. Moulia B, Fournier M. 2009 The power and control of gravitropic movements in plants: a biomechanical and system biology view. *J. Exp. Bot.* **60**, 461–486. (doi:10.1093/jxb/ern341)
4. Galland P. 2002 Tropisms of *Avena* coleoptiles: sine law for gravitropism, exponential law for photogravitropic equilibrium. *Planta* **215**, 779–784. (doi:10.1007/s00425-002-0813-6)
5. Morita MT. 2010 Directional gravity sensing in gravitropism. *Annu. Rev. Plant Biol.* **61**, 705–720. (doi:10.1146/annurev.arplant.043008.092042)
6. Morita MT, Tasaka M. 2004 Gravity sensing and signaling. *Curr. Opin. Plant Biol.* **7**, 712–718. (doi:10.1016/j.pbi.2004.09.001)
7. Tasaka M, Kato T, Fukaki H. 1999 The endodermis and shoot gravitropism. *Trends Plant Sci.* **4**, 103–107. (doi:10.1016/S1360-1385(99)01376-X)
8. Hashiguchi Y, Tasaka M, Morita MT. 2013 Mechanism of higher plant gravity sensing. *Am. J. Bot.* **100**, 91–100. (doi:10.3732/ajb.1200315)
9. Kolesnikov YS, Kretynin SV, Volotovsk ID, Kordyum EL, Ruelland E, Kravet VS. 2016 Molecular mechanisms of gravity perception and signal transduction in plants. *Protoplasma* **253**, 987–1004. (doi:10.1007/s00709-015-0859-5)
10. Silk WK. 1984 Quantitative descriptions of development. *Annu. Rev. Plant Physiol.* **35**, 479–518. (doi:10.1146/annurev.pp.35.060184.002403)
11. Bastien R, Bohr T, Moulia B, Douady S. 2013 Unifying model of shoot gravitropism reveals proprioception as a central feature of posture control in plants. *Proc. Natl Acad. Sci. USA* **110**, 755–760. (doi:10.1073/pnas.1214301109)
12. Pfeffer W. 1904 *Pflanzenphysiologie*, vol. 2. Leipzig, Germany: W. Engelmann.
13. Kutschera U. 2001 Gravitropism of axial organs in multicellular plants. *Adv. Space Res.* **27**, 851–860. (doi:10.1016/S0273-1177(01)00148-X)
14. Myers AB, Firn R, Digby J. 1994 Gravitropic sign reversal—a fundamental feature of the gravitropic perception or response mechanisms in some plant organs. *J. Exp. Bot.* **45**, 77–83. (doi:10.1093/jxb/45.1.77)
15. Digby J, Firn R. 1995 The gravitropic set-point angle (gsa): the identification of an important developmentally controlled variable governing plant architecture. *Plant Cell Environ.* **18**, 1434–1440. (doi:10.1111/j.1365-3040.1995.tb00205.x)
16. Sachs JV. 1887 *Lectures on physiology of plants*. Oxford, UK: Oxford University Press.
17. Firn R, Digby J. 1979 A study of the autotropic straightening reaction of a shoot previously curved during geotropism. *Plant Cell Physiol.* **38**, 1346–1353. (doi:10.1111/j.1365-3040.1979.tb00786.x)
18. Tarui Y, Iino M. 1997 Gravitropism of oat and wheat coleoptiles: dependence on the stimulation angle and the involvement of autotropic straightening. *Plant Cell Environ.* **2**, 149–154. (doi:10.1093/oxfordjournals.pcp.a029128)
19. Meskauskas A, Moore D, Novak Frazer L. 1998 Mathematical modelling of morphogenesis in fungi: spatial organization of the gravitropic response in the mushroom stem of *Coprinus cinereus*. *New Phytol.* **140**, 111–123. (doi:10.1046/j.1469-8137.1998.00252.x)
20. Stankovic B, Volkmann D, Sack FD. 1998 Autotropism, automorphogenesis, and gravity. *Physiol. Plant*. **102**, 328–335. (doi:10.1034/j.1399-3054.1998.1020222.x)
21. Fourcaud T, Lac P. 2003 Numerical modelling of shape regulation and growth stresses in trees: 1. An incremental static finite element formulation. *Trees* **17**, 23–30. (doi:10.1007/s00468-002-0202-6)
22. Goldstein RE, Goriely A. 2006 Dynamic buckling of morphoelastic filaments. *Phys. Rev. E* **74**, 010901(R). (doi:10.1103/PhysRevE.74.010901)
23. Senan NAF, O'Reilly OM, Tresierras TN. 2008 Modeling the growth and branching of plants: a simple rod-based model. *J. Mech. Phys. Solids* **56**, 3021–3036. (doi:10.1016/j.jmps.2008.06.005)
24. Moulton DE, Lessinnes T, Goriely A. 2013 Morphoelastic rods. Part 1: a single growing elastic rod. *J. Mech. Phys. Solids* **61**, 398–427. (doi:10.1016/j.jmps.2012.09.017)
25. O'Reilly OM, Tresierras TN. 2011 On the evolution of intrinsic curvature in rod-based models of growth in long slender plant stems. *Int. J. Solids Struct.* **48**, 1239–1247. (doi:10.1016/j.ijsolstr.2010.12.006)
26. Bastien R, Douady S, Moulia B. 2014 A unifying modeling of plant shoot gravitropism with an explicit account of the effects of growth. *Front. Plant Sci.* **5**, 136. (doi:10.3389/fpls.2014.00136)
27. Cosgrove DJ. 1997 Assembly and enlargement of the primary cell wall in plants. *Annu. Rev. Cell Dev. Biol.* **13**, 171–201. (doi:10.1146/annurev.cellbio.13.1.171)
28. Niklas KJ. 1992 *Plant biomechanics: an engineering approach to plant form and function*. Chicago, IL: University of Chicago Press.

Supplementary Information: On the growth and form of shoots

Raghunath Chelakkot[†‡], L. Mahadevan[†*]

[†]*Paulson School of Engineering and Applied Sciences,*

Harvard University,

Cambridge, MA 02138, USA.

[‡]*Department of Physics,*

Indian Institute of Technology Bombay,

Mumbai 400076, India.

[*]*Departments of Organismic and Evolutionary Biology and of Physics,*

Wyss Institute for Biologically Inspired Engineering,

Kavli Institute for Nano-bio Science and Technology,

Harvard University,

Cambridge, MA 02138, USA.

I. INFLUENCE OF RELATIVE MATURATION RATE

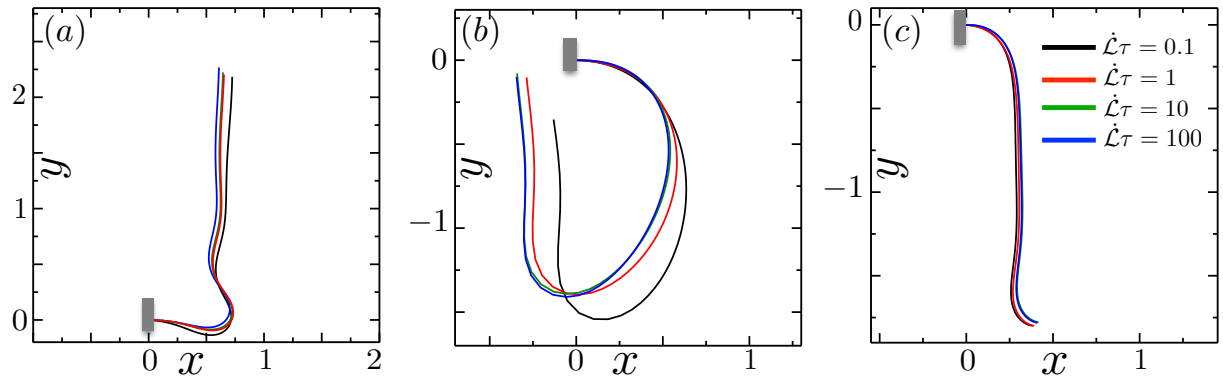

FIG. SI-1: Comparing the shapes of a growing filament for various values of relative maturation rate, $\dot{\mathcal{L}}\tau$ for sensitivity parameter $\mathcal{S} = 5$ and for three values elasticity parameter, (a) $\mathcal{E} = 1.14$,(b) $\mathcal{E} = 1.26$ and (c) $\mathcal{E} = 1.52$.

Here we examine the influence of the maturation rates on the growth morphologies in plant shoots. The relative maturation rate is controlled by the parameter $\dot{\mathcal{L}}_0\tau$ which we allow to vary in the range $[0.1 - 100]$. In Fig.SI-1 we show the observed shapes for various values of $\dot{\mathcal{L}}_0\tau$ and the elasticity parameter $\mathcal{E}$ for the sensitivity $\mathcal{S} = 5$, obtained by solving (2.4)-(2.7) of the main text. As $\mathcal{S}$ is relatively large, the actual shape of the shoots will influence the time dependent growth and the differences due to variations in $\dot{\mathcal{L}}_0\tau$ are expected to get amplified at long time.

However, there are no significant variations in the qualitative morphologies seen, even though there are quantitative differences.

II. INFLUENCE OF RELATIVE GROWTH ZONE LENGTH

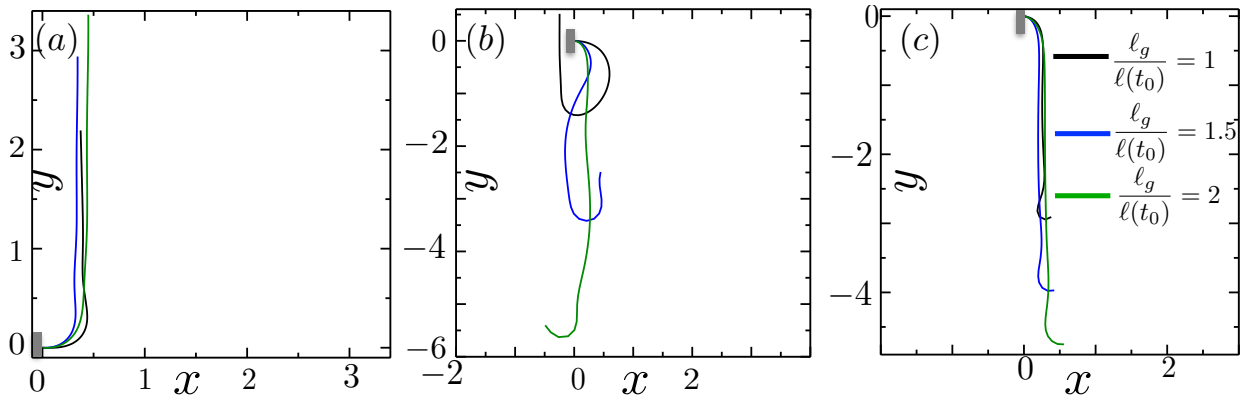

FIG. SI-2: The shapes of a growing filament for different relative length of growth zone $\ell_g/\ell(t_0)$. (a) Negative gravitropism for sensitivity parameter $\mathcal{S} = 5$ and elasticity parameter $\mathcal{E} = 0.7$. (b) Model shoot showing gravitropic sign reversal. The parameter regime where this behavior is observed varies depending on $\ell_g/\ell(t_0)$. (top to bottom) $\mathcal{S} = 5$, $\mathcal{S} = 6$, $\mathcal{S} = 7$ and for $\mathcal{E} = 1.3$. (c) Positive gravitropism observed for $\mathcal{E} = 1.52$ and $\mathcal{S} = 5$.

To test the dependence of the shapes of growing shoots on the value of the length of growing zone, ℓ_g relative to the initial length of the shoot, we chose various values of $\ell_g/\ell(t_0)$. Since the initial condition is always assumed to be a young shoot, we only consider cases with $\ell_g \geq \ell(t_0)$. Fig. SI-2 shows the results obtained for values of $\ell_g/\ell(t_0) = 1, 1.5$ and 2. The simulations show that the shoot basically displays same morphologies for all three values of ℓ_g. When the gravitropic sensitivity $\mathcal{S}$ dominates, the shoots always display negative gravitropism (Fig. SI-2(a)), whereas when elasticity parameter $\mathcal{E}$ dominates, they display positive gravitropism (Fig. SI-2(c)). When both these parameters are equally significant, the shoots display gravitropic reversal (Fig SI-2(b)). However, the parameter values where this reversal is observed shift to larger values with an increase in ℓ_g. Therefore, we again conclude that the qualitative features of the morphospace are independent of the value of ℓ_g, although the parameter values for which the shape transition occurs vary for large $\mathcal{E}$ and $\mathcal{S}$.

III. SIMULATION MOVIES

MOVIE1: Negative gravitropism observed in the massless limit for $\mathcal{S} = 2.5$, and $\mathcal{E}$=0

MOVIE2: Reversal of growth direction for $\mathcal{S} = 2.5$, and $\mathcal{E}$=1

MOVIE3: Reversal of growth direction for $\mathcal{S} = 3$, and $\mathcal{E}$=1.2

MOVIE4: Effectively positive gravitropism observed for $\mathcal{S} = 3$, and $\mathcal{E} = 1.5$.

The movies show the growing shoot for different values of the sensitivity parameter $\mathcal{S}$, and the elasticity parameter $\mathcal{E}$. The green color corresponds to the young, soft shoot while the brown color corresponds to the older stiffer shoot.